

3-D Computational Modeling of RF MEMS Switches

H. D. Espinosa, M. Fischer, Y. Zhu and S. Lee

Dept. of Mechanical Engineering, Northwestern University, Evanston, IL 60208-3111, USA,
espinosa@northwestern.edu

ABSTRACT

Young's modulus and residual stress state of freestanding thin membranes are characterized in this work by means of wafer level experimental techniques. RF MEMS Switches manufactured by Raytheon Systems Co. are investigated using a new method that combines a Membrane Deflection Experiment (MDE) and numerical simulations. It is found that the thin aluminum alloy membranes used in the RF MEMS devices have a Young's modulus of 70 ± 10 GPa in the plane of the membrane, and a residual tensile stress of 4 ± 1 MPa. The accuracy of the identified parameters is confirmed by sensitivity studies to geometric aspects of the specimens and loads. It is found that changes in initial residual stress affect the load-deflection curves at small values of deflection. By contrast, variations in Young's modulus result in changes in load-deflection curvature at large displacements. These features are very important to decouple both effects in the process of identification of the parameters.

Keywords: MEMS, Computational Mechanics, Experimental Mechanics, Elasticity, Radio Frequency.

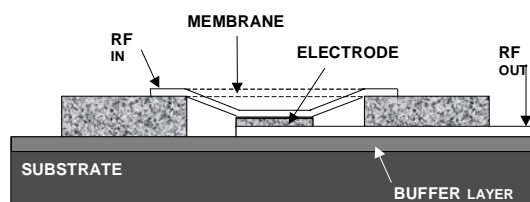
1 INTRODUCTION

RF switching using MEMS technology has been carried out by Peterson, 1979[1], Zavracky and Morrison, 1984[2], Yao and Chang, 1995[3], and Larson et al., 1991[4], using ohmic contact. The development of RF MEMS switches using metal membranes with capacitive coupling has been reported by Goldsmith et al., 1998[5], 1999[6] with low insertion loss, reasonable switching voltages, fast switching speeds and excellent linearity. For space systems and areas in which size and weight are crucial, microfabrication techniques are rapidly capturing the market. Radar technology and wireless communications are examples of common applications of RF MEMS switches.

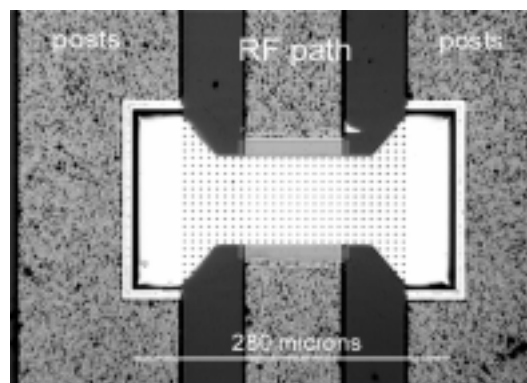
For this kind of circuits, Raytheon Systems Co. developed MEMS switches to operate in tunable filters and oscillators used as varactors (tunable capacitors). The structure of one MEMS switch is schematically shown in Figure 1. The devices are manufactured on a GaAs substrate, over which the "bow-tie" metal membrane is deposited by evaporation. The material used in the

membrane is an Aluminum alloy. This membrane is the only moving part of the device. Its shape, size and mechanical properties determine the behavior of the MEMS switch. Two of its edges are attached to thin posts that maintain it suspended over an electrode. The switch itself is able to operate at very high frequencies, as a result of its low inertia. Switching is achieved by pulling in the membrane to the bottom electrode. The metal dielectric avoids the two components to become in ohmic contact, preventing sticking and/or microwelding. It also causes the RF signal to capacitively couple from the upper membrane to the lower electrode. Typical switching time is approximately $5 \mu\text{s}$.

This paper addresses the identification of Young's modulus and residual stress state of the freestanding RF thin membranes. A new methodology that combines a Membrane Deflection Experiment (MDE) and 3-D numerical



(a)



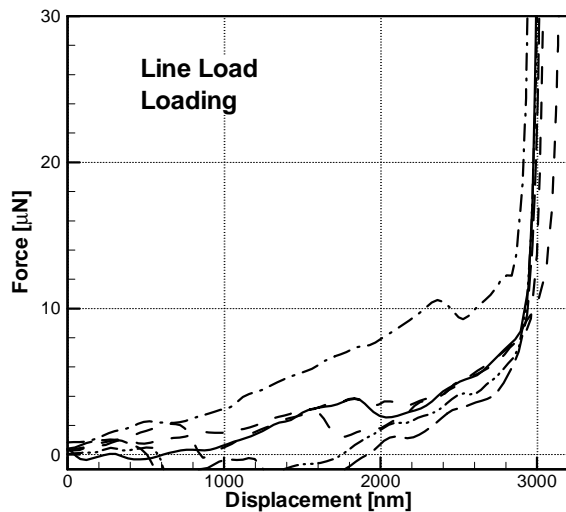
(b)

Figure 1: (a) Cross section of RF MEMS switch manufactured by Raytheon Systems Co. (b) Top view of the "bow-tie" membrane mounted on posts. It is made of an aluminum alloy and contains a pattern of holes for membrane release during microfabrication.

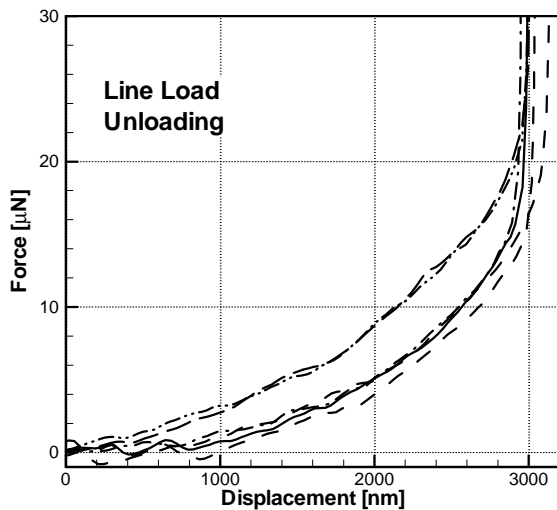
simulations is discussed. The former consists in the measurement of load versus center membrane deflection using specially designed diamond tips and a nanoindenter. The later are 3-D numerical simulations of the membrane deflections using shell elements and multi-body contact algorithms.

2 MEMBRANE DEFLECTION EXPERIMENTS

Making use of a nanoindenter, a membrane deflection experiment is performed to investigate the membrane structural response. The technique should not be confused with nanoindentation or with micro bending of cantilevers,



(a)



(b)

Figure 2: (a) Loading part of MDE in new generation membranes, using line load. The snap-through in the curve is a very interesting feature observed later on in simulations. (b) Unloading part of MDE in new generation membranes, using line load. Repeatability is evident.

see previous work by Nix et al., Ref. [7]. Since the sample is attached to the posts along two of its edges, and a gap exists under the membrane, a wedge-tip is used to deform the membrane elastically. The experiment consists in applying a line load at the center of the fixed-fixed membrane. A specially designed diamond wedge-tip 115 microns long was used to apply the line load. Pushing the membrane down tests the specimen structural response providing information on its elastic behavior and residual stress state. In this manner, simple tension of the membrane is achieved except for boundary bending effects.

Experimental results obtained by examining 6 switches in loading and unloading are shown in Figure 2. Contact with the membrane is taken as the zero displacement. As previously explained, the membrane response to stretching is obtained, as it is pulled down by a displacement equal to the gap. Then, the bottom electrode is reached and a steep change in the curve, corresponding to a large stiffness increase, is observed. An interesting feature is the shape of the loading curves. A kink at particular load levels is observed in the six loading curves plotted in Figure 2 (a). A smooth behavior is observed in the unloading part of the load-displacement curve, Figure 2 (b). Spontaneous snap-through of the membranes originates significant changes in stiffness at some point during loading. This phenomenon is attributed to shape instability related to initial membrane waviness and curvature. It is clear that snap-through occurs at different deflections for different membranes. This is consistent with the fact that the initial membrane shape varies from switch to switch. Similar experimental results were obtained when a concentrated force, using a Berkovich tip, was applied in the middle of the span, Fischer, 1999 [8].

3 FINITE ELEMENT MODELING

The analysis was conducted using ABAQUS Implicit, version 5.7. All cases were run using flat meshes, curved in x only or double curved. The curved shapes will be called x-shaped and xy-shaped, respectively. The detail in Figure 3 clearly shows the double curvature of the mesh in this case and the refinement of the elements in the area of contact. This is important to assure the convergence of the iterations, which is checked by the software.

The membrane is discretized using 8-noded 2D shell elements with variable sizes in the x-y plane, preserving the membrane geometry, and constant thickness of 300 nm in the z-direction. This thickness is used for the calculation, although the elements are 2D, which is valid when modeling a thin shell in ABAQUS. The selected element for the membrane is the S8R5. The first letter in its nomenclature indicates that it is a stress/displacement shell type of element, used only for thin shells. The number 8 indicates the number of nodes. R stands for reduced integration, which means that a lower-order integration is

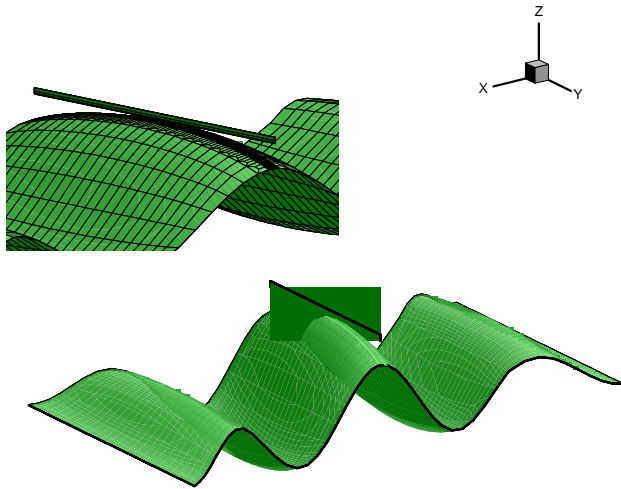


Figure 3: Initial shape of the membrane for line load case. Refinement of the mesh is shown in the detail.

used to calculate the element stiffness. Reduced integration provides more accurate results when elements are not distorted, and significantly reduces running time. The number 5 is optional, and it indicates five degrees of freedom. In these computations, ABAQUS automatically change the S8R5 for the nine-node S9R5 in the slave surface of the contact pair. Plane stress was used in all cases.

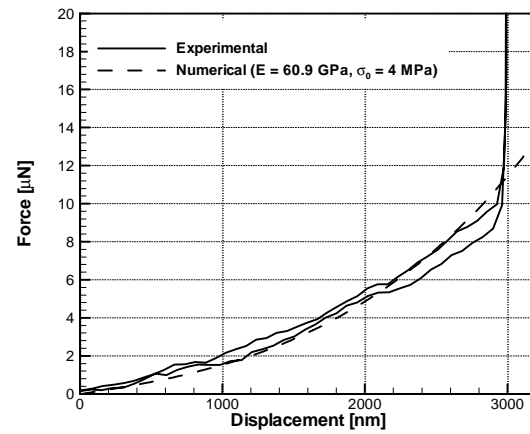
The diamond wedge-tips have a radius of 40 nm and 80-degree incline angles. For the different geometries, the 115-micron tip covers the whole width of the membranes. The element type R3D4 was employed in all cases. All the nodes that form the tip are referred to a particular node, to which the displacement in the z-axis is prescribed. The rigid element nodes are master nodes in the contact pair, meaning that stresses and strains are not calculated for these elements. On the other hand, the shell elements used for the membrane define the slave surface, which can be solved for stresses and deformations.

The contact pair interaction is divided into two loading steps. Only a displacement in the z direction is applied to the indenter. This displacement increases linearly with the time increments. The first step is to put the two bodies in mechanical contact and to achieve equilibrium of residual stresses, which results in a change of membrane shape. The indenter goes from zero displacement to -0.01 microns, and the step ends when contact is made. The second step starts at that point, and it consists in continuing the motion until a total displacement of -3.5 microns is reached.

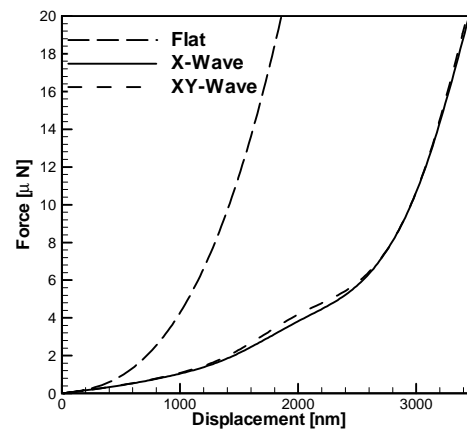
One of the main findings from this investigation is that variations in residual stress and membrane elastic properties affect the load-deflection curve in different regimes. In fact, changes in initial residual stress significantly affect the load-deflection slope at small values of deflection. By contrast, variations in Young's modulus result in changes in load-deflection slope at large

displacements. These features are very important to decouple both effects in the identification process. This novel technique has the potential to examine plasticity and failure mechanisms of MEMS films at the nano-scale. Figure 4 (a) shows a plot matching simulations and MDE experimental results in the case of point load configuration, Berkovich tip. The simulation corresponds to a material Young's modulus of 60 GPa and an initial residual stress of 4 MPa.

Another major finding in this investigation is that initial membrane shape significantly influences the load-deflection curve during the first loading/unloading cycle. Because of differences in materials thermal expansion coefficients and device geometry, the membrane has a well-defined initial geometry. For the purpose of investigating this effect, a shape function was identified using atomic force microscopy. This function was then used to described initial membrane shapes in a numerical investigation. Our



(a)



(b)

Figure 4: (a) Comparison of the numerical result with experimental data. (b) Force-deflection curve for three different initial membrane shapes.

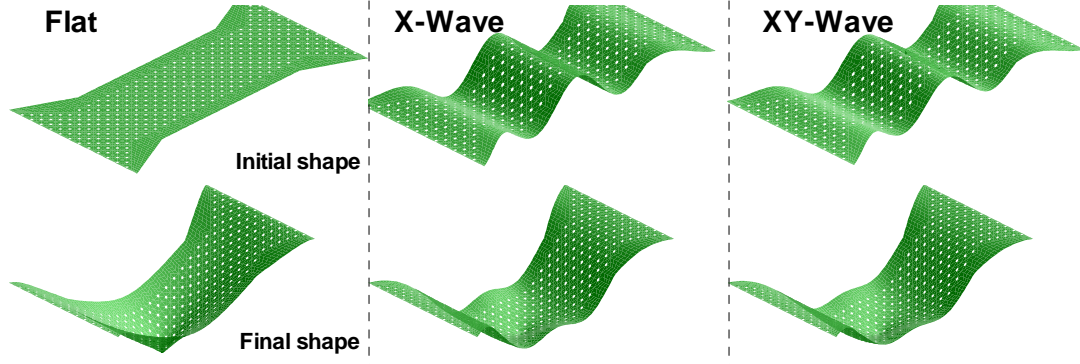


Figure 5: Shape of the membranes considered in the analysis. Membrane z-displacement is amplified for the purpose of visualization.

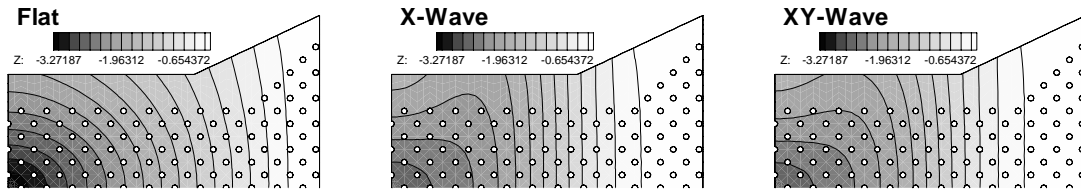


Figure 6: Contours of deflection at maximum load for each one of the three cases, flat, x-wave and xy-wave membranes.

systematic study demonstrates that when the membrane has initial deflections, it may introduce structural instabilities, which cannot be neglected. Figure 4 (b) shows the load-deflection curve for the three cases, flat, x-waved and x-y waved, when the initial residual stress is zero. The membrane curvature observed in the single and double wave initial shapes are clearly observed. Figure 5 shows the membrane shapes at the beginning of the analyses and at maximum load. Figure 6 shows the contours of the maximum deflection for the three initial membrane shapes under investigation. In all these simulations, a Berkovich (pyramidal) tip was used. We have also investigated wedge-tips (line loads). The results from these investigations will be reported in the final manuscript and conference presentation.

4 CONCLUSION

A combined experimental-computational approach was developed to examine elastic and residual stress state in RF-MEMS switches.

Our investigation of switches manufactured by Raytheon Systems Co. resulted in the identification of a Young's Modulus of 70 ± 10 GPa and a residual stress of 4 ± 1 MPa.

ACKNOWLEDGEMENTS

The authors wish to thank Raytheon Systems Co. and NSF for funding this research. A special thank is due to S. Chen, T. Baughn and C. Goldsmith for their input during this investigation.

REFERENCES

- [1] K. Peterson, "Micromechanical Membrane Switches on Silicon", IBM J. Res. Develop., 23, 376-385, 1979.
- [2] P. Zavracky and R. Morrison, Proc. of IEEE Solid State Sensor Conference, 1984.
- [3] J. Yao and M. Chang, Transducers'95, 384-387, 1995.
- [4] L. Larson, R. Hackett, M. Melendes and R. Lohr, IEEE Microwave Theory Tech. Symp., 27-30, 1991.
- [5] C. Goldsmith, Z. Yao, S. Eshelman and D. Denniston, IEEE Microwave and Guided Wave Letters, 8, 269-271, 1998.
- [6] C. Goldsmith, A. Malczewski, Z. Yao, S. Chen, J. Ehmke and D. Hinzl, International Journal of RF and Microwave Computer-Aided Eng., 9, 362-374, 1999.
- [7] S. Baker and W. Nix, J. of Materials Research, 9, 3131-3144, 1994.
- [8] M. Fischer, Master Thesis, Purdue University, West Lafayette, IN, 1999.